Diurnal and seasonal variability of surface ozone and NO_x at a tropical coastal site: Association with mesoscale and synoptic meteorological conditions

Liji Mary David[1] and Prabha R. Nair[1]

Received 17 September 2010; revised 2 February 2011; accepted 10 February 2011; published 18 May 2011.

[1] Simultaneous measurements of near-surface ozone, NO_x ($NO + NO_2$), and meteorological parameters were carried out at the tropical coastal location of Trivandrum (8.55°N, 77°E) in India from November 2007 to May 2009. The data have been used to investigate the diurnal and seasonal patterns of ozone and its precursor, NO_x, and also the interdependence of these two chemical species. The diurnal pattern is found to be closely associated with the mesoscale circulation (sea breeze and land breeze) and the availability of NO_x. The daytime peak in ozone extends until the onset of land breeze, which brings in NO_x for titration of ozone. Near-surface ozone concentration reaches peak values during the postmonsoon or winter months and shows minima during the summer or monsoon season. The high ozone concentration during winter is due to the presence of northeasterly winds that transport precursor gases to the site. The daytime concentration of ozone is found to be directly linked to the nighttime level of NO_x. The present analysis reveals that one molecule of NO_x or NO_2 is responsible for the formation of about seven to nine molecules of ozone. A study of satellite-derived tropospheric ozone and total ozone has shown that tropospheric ozone contributes 8%–15% of total ozone over this site and near-surface ozone contributes 34%–83% of tropospheric ozone. The seasonal pattern of tropospheric column ozone is similar to that of tropospheric NO_2.

Citation: David, L. M., and P. R. Nair (2011), Diurnal and seasonal variability of surface ozone and NO_x at a tropical coastal site: Association with mesoscale and synoptic meteorological conditions, *J. Geophys. Res.*, *116*, D10303, doi:10.1029/2010JD015076.

1. Introduction

[2] Tropospheric ozone is a crucial constituent which determines the chemical transformations and lifetimes of several trace gases in the troposphere [*Levy*, 1971; *Weinstock and Niki*, 1972; *Wofsy et al.*, 1972; *Crutzen*, 1995]. It is responsible for the production of the highly reactive OH radical, which oxidizes and removes the majority of pollutants from the atmosphere [*Levy*, 1971; *Carpenter et al.*, 1997]. Through the absorption of infrared radiation at 9.6 μm, ozone also acts as a greenhouse gas, which has implications for the global climate. Even though the warming effect of ozone is small compared to gases such as CO_2, methane, and water vapor, at ~0.35 W m^{-2}, it is still significant [*Intergovernmental Panel on Climate Change*, 2007]. Ozone is also an environmental pollutant with adverse effects on human health and vegetation [*Heck et al.*, 1982; *Reich and Amundson*, 1985; *Chameides et al.*, 1994, 1999a, 1999b; *Lee et al.*, 1996; *Finnan et al.*, 1997; *World Health Organization*, 2000].

[3] In the troposphere, ozone is formed by two major mechanisms, namely, (1) intrusion from stratospheric altitudes through large-scale or mesoscale eddy diffusion or through meridional or zonal transport processes [*Danielsen*, 1959; *Reiter*, 1975] and (2) photochemical production [*Crutzen*, 1974; *Chameides and Walker*, 1976; *Fishman et al.*, 1979]. Photochemical production of tropospheric ozone involves the oxidation of CO, CH_4, nonmethane hydrocarbons (NMHCs), and other volatile organic compounds (VOCs), depending on the concentrations of NO_x ($NO + NO_2$) and hydrogen oxide radicals (OH and peroxy radicals), which act as catalysts in the reaction [*Fishman and Crutzen*, 1977; *Chameides*, 1978; *Crutzen et al.*, 1979, 1985, 1999; *Logan et al.*, 1981]. Biomass burning, fossil fuel combustion, and other anthropogenic activities generate CO, CH_4, VOCs, etc., which are oxidized to ozone in a NO_x-rich environment. The main sources of NO_x are fossil fuel combustion, biomass burning, soil microbial activity, and lightning. NO plays a critical role in ozone production, even in rural regions, where NO concentration is higher than 10 parts per trillion (ppt) [*Lin et al.*, 1988]. The amount of tropospheric ozone generated by the pho-

[1]Space Physics Laboratory, Vikram Sarabhai Space Centre, Trivandrum, India.

0148-0227/11/2010JD015076

tochemical reactions of chemical pollutants is much larger than the influx of ozone from the stratosphere [*Crutzen*, 1995; *Crutzen et al.*, 1999].

[4] Ozone is destroyed by either dry deposition or photochemical loss mechanisms. The most efficient loss mechanism is the reaction with water vapor [*Chameides and Walker*, 1976; *Fishman and Crutzen*, 1978]. To a great extent, the lifetime of ozone is determined by the amount of water vapor (a source of OH radical) and solar radiation [*Fishman et al.*, 1991; *Michelsen et al.*, 1994]. The amount of ozone destroyed through photochemical loss mechanisms is several times greater than that destroyed as a result of surface deposition [*Ripperton and Vukovich*, 1971].

[5] Meteorology also plays an important role in the formation, dispersion, transport, and dilution of ozone in the atmosphere [*Comrie and Yarnal*, 1992; *Vukovich*, 1994, 1995; *Dueñas et al.*, 2002; *Elminir*, 2005; *Tu et al.*, 2007]. Type of air mass is another important factor in assessing the ozone concentration on a regional scale [*Naja et al.*, 2003; *Tu et al.*, 2007]. The seasonal and diurnal variations of surface ozone and its precursors and the related meteorology have been extensively studied around the world, particularly in Europe [*Danalatos and Glavas*, 1996; *Cárdenas et al.*, 1998; *Chatterton et al.*, 2000; *Dueñas et al.*, 2002] and North America [*Aneja et al.*, 1997; *Olszyna et al.*, 1997; *Raddatz and Cummine*, 2001; *Lehman et al.*, 2004]. A few reports on the temporal features of ozone and related gas pollutants are also available from sites in China and Japan [*Jaffe et al.*, 1996; *Wang et al.*, 2001; *Chou et al.*, 2006; *Tu et al.*, 2007]. However, long-term measurements of surface ozone over tropics where photochemistry is strongest are scarce. The diurnal and seasonal variations of surface ozone have been reported from a few sites in India [*Khemani et al.*, 1995; *Lal et al.*, 2000; *Naja and Lal*, 2002; *Nair et al.*, 2002; *Debaje et al.*, 2003; *Naja et al.*, 2003; *Jain et al.*, 2005; *Beig et al.*, 2007; *Ghude et al.*, 2008; *Reddy et al.*, 2008; *Kumar et al.*, 2010]. These studies have indicated significant spatial heterogeneities in ozone distribution.

[6] This paper presents observations and analysis of the diurnal and seasonal variations in surface ozone in association with its precursors, nitrogen oxides (NO_x = NO + NO_2), and the meteorological conditions at a tropical coastal station, Trivandrum (8.55°N, 77°E, 3 m above sea level), as recorded during the period November 2007 to May 2009. First-cut results on the temporal behavior of near-surface ozone at this location have already been published by *Nair et al.* [2002]. The major focus of the present study is on the interdependence of ozone and its major precursor, NO_x, which was not addressed by *Nair et al.* [2002]. It may be noted that NO_x measurements from this location are reported here for the first time. Moreover, this paper clearly establishes the role of mesoscale meteorological features like sea breeze (SB) and land breeze (LB) in relationship to the diurnal variations of ozone as well as NO_x (which was not discussed by *Nair et al.* [2002]) and the role of synoptic-scale airflow in their seasonal patterns. In addition, the seasonal variations in tropospheric ozone, NO_2, and column ozone were also examined by making use of satellite-based data. Estimates of the contribution of surface ozone to the tropospheric column and that of tropospheric ozone to the total column ozone are also presented.

2. Observation Site and General Meteorology

[7] The observation site, Trivandrum, is situated on the southwest coast of India ~500 m from the Arabian Sea, and the coastline lies along the 145°–325° azimuth. The geographic location of the site along with a site map of the study area is shown in Figure 1. The city of Trivandrum, with a population of 744,983 (http://www.censusindia.gov.in), lies east-southeast of the observation site about 10 km away. The site is characterized by a fairly flat and sandy terrain and is devoid of any large-scale industrial activity.

[8] Figure 2 shows the variation of monthly total rainfall along with the mean relative humidity (RH) and temperature (T) during the study period. Figure 3 shows the monthly mean airflow pattern at 925 hPa in the 0°–25°N and 55°E–95°E sector surrounding the observation site (marked by a black dot) for the year 2008, as obtained from the National Centers for Environmental Prediction/National Center for Atmospheric Research reanalysis (http://www.esrl.noaa.gov/psd/data/gridded/reanalysis/). The most prominent meteorological phenomenon at this site is the Asiatic monsoon, which sets in by the first week of June [*Asnani*, 1993]. During the first phase of the monsoon season (June–August), synoptic winds are stronger, the circulation is southwesterly-westerly (from ocean to land), and the observation site experiences heavy rainfall. The wind and rainfall weaken by August or September, and by October or November the wind direction changes to northeasterly. The wind direction continues to be northeasterly until February, when the flow is mostly from the continent. The annual rainfall at this location is ~1800 mm, and on average, 75% of the rainfall occurs between June and November, with <3% occurring in December, January, and February. There are moderate showers (~20%) from March through May, when air temperature is highest and winds are in transition from northeasterly to southwesterly (Figure 3). December, January, and February are characterized by low temperatures, relatively dry atmospheric conditions, and insignificant rainfall. On the basis of the major synoptic meteorological conditions discussed above, a year is divided into four seasons: winter (December–February), summer or premonsoon (March–May), summer monsoon or monsoon (June–August), and winter monsoon or postmonsoon (September–November).

3. Experimental Technique and Data

[9] Continuous measurement of near-surface ozone was carried out by using an online UV photometric ozone analyzer (model 49C, Thermo Electron Corporation, USA). This instrument operates on the principle of absorption of UV light by the ozone molecules at a wavelength of 254.7 nm. Calibration of the instrument is done regularly by the built-in ozonator (ozone generator) and zero air generator. The lower detection limit of the instrument is 1.0 ppb. Air samples are drawn at a height of ~3 m through a 5 μm PTFE filter attached to the instrument through a Teflon tube with an outer diameter of one quarter inch. The instrument takes measurements at intervals of ~10 s, and data averaged at

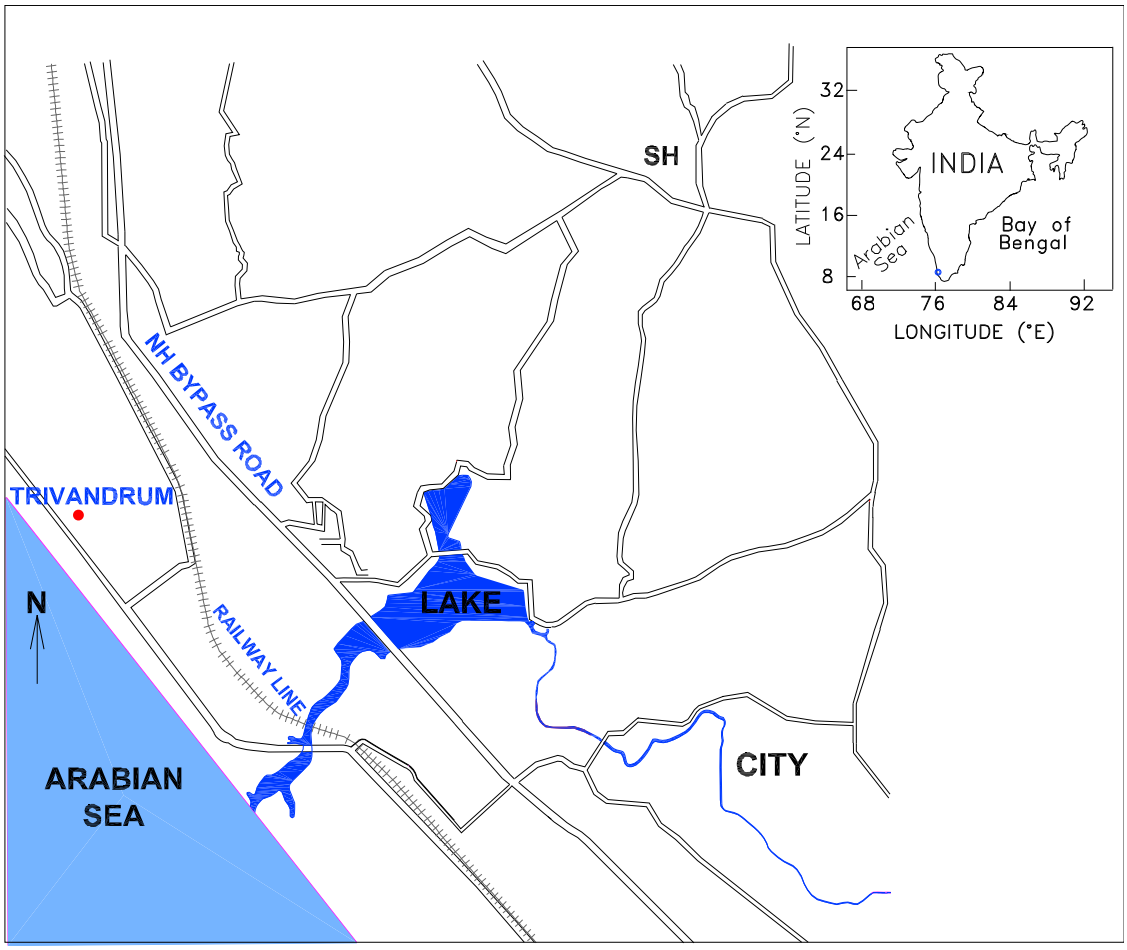

Figure 1. The geographic location of the site along with a site map of the study area.

5 min intervals were used in the present study. Simultaneous measurements of nitrogen oxides (NO, NO_2, and NO_x) were also carried out at 5 min intervals with a chemiluminescence NO_x analyzer (model ML® 9841B, Monitor Europe) from November 2007 to May 2009. The instrument works on the principle of gas phase chemiluminescence and performs continuous analysis of nitric oxide (NO), total oxides of nitrogen (NO_x), and nitrogen dioxide (NO_2). The instrument has a resolution of 0.5 ppb and a response time of 10 s. However, because of frequent rain showers, instruments could not be operated continuously during September and October 2008. Hence, records of complete diurnal cycles are available for only 4–5 days, even though daytime measurements are available for 12 days. For all other months 10–15 days of data are available. Meteorological parameters such as temperature, relative humidity, rainfall, wind speed, and wind direction were obtained at 5 min intervals from an automatic weather station operating at the observation site.

[10] With a view toward broadening understanding of the contribution of near-surface ozone to tropospheric ozone and of tropospheric contribution to total column ozone, satellite measurements have also been used in this study. Currently, the data collected by the Ozone Monitoring Instrument (OMI) and the Microwave Limb Sounder (MLS) on board the EOS Aura satellite provide global coverage of ozone measurements. OMI provides global coverage of a single day, with nadir viewing and scanning back and forth in the orbit track. MLS looks forward along its orbit track, and measurements that are almost spatially coincident are made by OMI and MLS with a time difference of <10 min. OMI has a pixel size of 13 × 24 km^2 at nadir and a swath width of 2600 km. Total column ozone is derived from OMI using the Total Ozone Mapping Spectrometer (TOMS) algorithm (version 8.5). MLS provides measurements of stratospheric column ozone by the standard method of pressure integration of ozone volume mixing ratio (version 2.2). Tropospheric column ozone is determined using the residual method, which involves subtracting measurements of MLS stratospheric column ozone from OMI total column ozone after adjusting for the intercalibration differences of the two instruments using the convective cloud differential method [*Ziemke et al.*, 2006]. Total ozone with a resolution of 0.25° × 0.25° can be obtained online at http://toms.gsfc.nasa.gov/pub/omi/data/Level3e/ozone, and tropospheric ozone with a resolution of 1° latitude × 1.25° longitude is archived at ftp://jwocky.gsfc.nasa.gov/pub/ccd/data_monthly_new. The precision uncertainty for derived gridded ozone is 5 Dobson units (DU) (7 ppbv), with a mean offset of 2 DU (OMI and MLS) [*Ziemke et al.*, 2009]. OMI also provides the tropo-

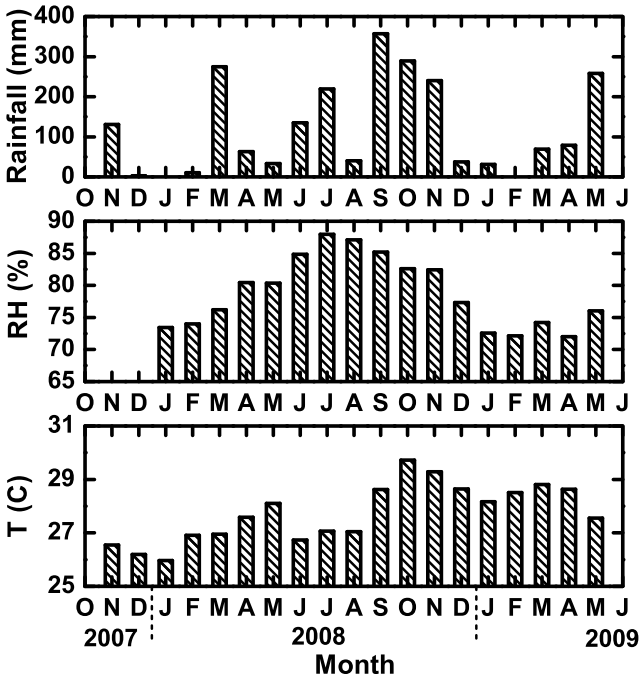

Figure 2. The variation of monthly total rainfall along with mean relative humidity (RH) and temperature (T) for November 2007 to May 2009.

spheric NO_2 column data, which are available daily with a resolution of 0.25° × 0.25° (level 3, gridded) at http://avdc.nasa.gov/. The tropospheric column NO_2 is underestimated by 15%–30% [*Celarier et al.*, 2008].

4. Results and Discussions

4.1. Diurnal Variations in Ozone and NO_x

[11] Ozone shows a systematic and consistent diurnal variation with a daytime high and a nighttime low. Figure 4a shows the typical diurnal pattern of ozone concentration at the observation site, averaged over 10 days during winter. Ozone concentration increases from 0700 LT (throughout this paper local time corresponds to Indian Standard Time), reaching a peak value of ~40 ppb at ~1000 LT, remaining more or less steady until ~1900 LT, and then decreasing to a low value of ~9 ppb late at night. Figures 4b–4d show the diurnal patterns of NO, NO_2, and NO_x, respectively, corresponding to the same periods. The NO_2 concentration lies in the range of 0.5–1 ppb during daytime, increases to 6 ppb during nighttime (~2200 LT), and remains high until early morning. The NO concentration is very low, ranging from 0 to ~1 ppb, with the highest values occurring late at night and in the early morning (~3 ppb). Diurnal patterns of NO_x and NO_2 are similar. The nighttime increase in NO is gradual compared to that of NO_2. Figures 4a and 4d clearly illustrate the anticorrelation between ozone and NO_x. Superposed on the diurnal pattern of NO_x, a sharp peak in NO_x is seen at ~0800 LT, which could be due to the fumigation effect, a widely discussed phenomenon in the context of dispersion of pollutants [*Stull*, 1988]. This effect is not seen in the case of ozone, as it gets depleted during the early evening hours.

[12] The diurnal variations in near-surface ozone concentration depend mainly on (1) photochemical reactions involving solar radiation and precursor gases of ozone; (2) boundary layer meteorological conditions, such as temperature and humidity or water vapor content; (3) changes in wind speed and direction, leading to the transport of ozone and/or its precursors; and (4) the effectiveness of surface (dry) deposition. Generally, the daytime increase in ozone concentration is attributed to the photochemical production of ozone from its precursor gases [*Fishman and Crutzen*, 1978; *Lin et al.*, 1988; *Crutzen et al.*, 1999]. In the present study, the role of NO_x, the most crucial precursor of ozone, in the evolution of the diurnal pattern is examined in detail.

[13] During daytime, photolysis of NO_2 takes place, leading to the formation of ozone as shown in the following reactions:

$$NO_2 + h\nu \rightarrow NO + O, \quad (1)$$

$$O + O_2 + M \rightarrow O_3 + M. \quad (2)$$

This subsequently leads to a decrease in NO_x concentrations. However, reactions (1) and (2) cannot account completely for the tropospheric ozone budget. Ozone is also produced through a series of reactions involving CH_4, NMHCs, other VOCs, CO, etc., which are initiated by OH radicals and are followed by the conversion of NO to NO_2. Photolysis of NO_2 gives rise to ozone, as reactions (1) and (2) demonstrate. During nighttime, the process of titration by NO_x reduces ozone levels as follows:

$$NO + O_3 \rightarrow NO_2 + O_2. \quad (3)$$

In general, the observed diurnal patterns of ozone and NO_x comply with these mechanisms. A detailed account of the interdependence of ozone and NO_x is given in section 4.3.

[14] Figures 4e–4h show the diurnal variation of the boundary layer meteorological parameters, namely, temperature, RH, wind speed, and wind direction, recorded for the same period as ozone and NO_x. It can be seen that increase in ozone concentration is positively associated with temperature, which, in turn, is negatively correlated with RH, as expected. However, the times of increase in ozone and temperature do not coincide exactly, with ozone increase lagging behind. Wind shows sharp changes in speed as well as direction around 0845 LT in the morning and 2000 LT in the evening. These changes correspond to the onsets of SB and LB, respectively. Section 4.4 gives a detailed account of the role of meteorological conditions and mesoscale circulation (SB and LB) in governing the diurnal variation of ozone and NO_x.

4.2. Seasonal Variations

[15] Almost all the diurnal patterns of ozone observed at this site reveal similar features, as shown in Figure 4a, with daytime high and nighttime low. However, the times of morning increase, evening decrease, and daily maximum as well as minimum values show variations over the course of a year. In order to understand the seasonal features, the diurnal patterns were examined on a monthly basis. Figure 5 shows the monthly averaged diurnal patterns of surface ozone (red) and NO_x concentrations (blue) for the study period. An analysis of these monthly mean diurnal patterns revealed certain seasonal features. The daytime ozone peak

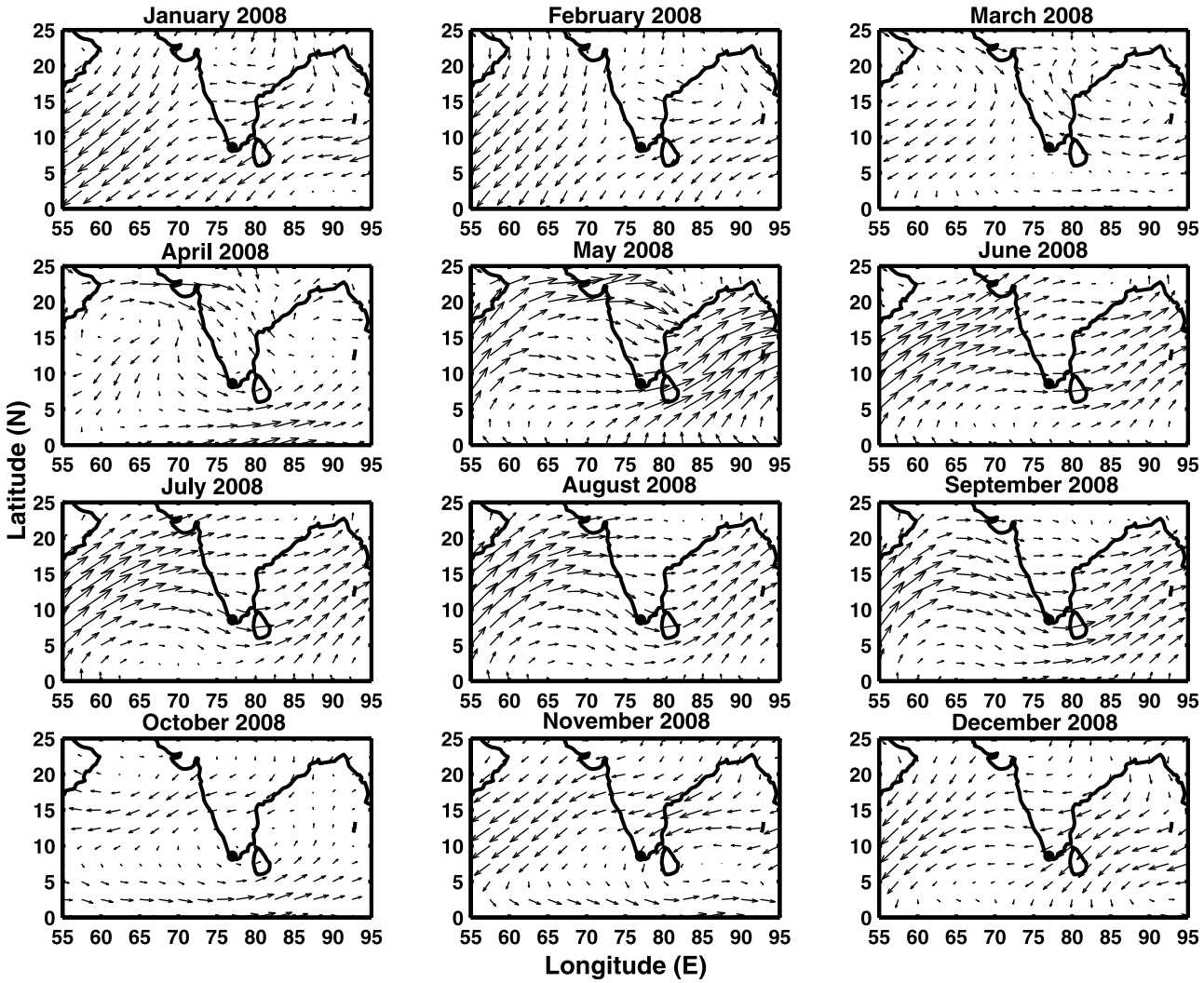

Figure 3. Mean airflow pattern at 925 hPa over the Indian region, obtained from the National Centers for Environmental Prediction/National Center for Atmospheric Research reanalysis for the year 2008. The black dot represents the observation site, Trivandrum.

is broader and peak values are higher from October through February (postmonsoon and winter months). Evening decrease in ozone is sharper during this period and is gradual and extended during summer and monsoon months (March–August). The monsoon months are characterized by low ozone concentration and short duration of peak. It was also seen that NO_x remains high during night and early morning hours and gets depleted after sunrise. In any month the decrease in NO_x coincides with the increase in ozone. The fumigation peak observed in NO_x during the early morning hours is more prominent from October to May. This could be due to the fact that convective activities become active after monsoon and are strongest during the summer. The amount of pollutants trapped above the nocturnal boundary layer could be greater during this period. Moreover, the prevailing winds being northeasterly (from October to February or March), transport of pollutants is also at its highest. In fact, the peak diminishes in amplitude or vanishes during the monsoon months.

[16] The seasonal mean daytime ozone concentration and that of nighttime NO_x are shown in Figures 6a and 6b, respectively, and a positive correlation is seen between the two. From Figures 5 and 6, it is clear that daytime ozone concentration as well as nighttime NO_x both peaked in the postmonsoon or winter months (DJF). During monsoon season, the lowest levels of both ozone and NO_x were observed, with peak values of 20–23 ppb and 2–3 ppb, respectively. However, the daytime concentration of NO_x was ~1 ppb and was comparable for all seasons, as in the case of nighttime ozone. These seasonal variations can be associated with changes in synoptic wind patterns, prevailing air mass type, and seasonal differences in solar irradiance. From October until February, when ozone concentration is high, the wind flow is easterly or northeasterly and directed from the inland locations (Figure 3). Figure 7 shows the 7 day air mass back trajectories reaching the location at 200 m (within the boundary height) at 0600 UT obtained using the Hybrid Single-Particle Lagrangian Integrated Trajectory (HYSPLIT) model for the year 2008 (R. R. Draxler and G. D. Rolph, 2003, http://ready.arl.noaa.gov/HYSPLIT.php). During October to February, the air mass trajectories originated from the northeast and traversed

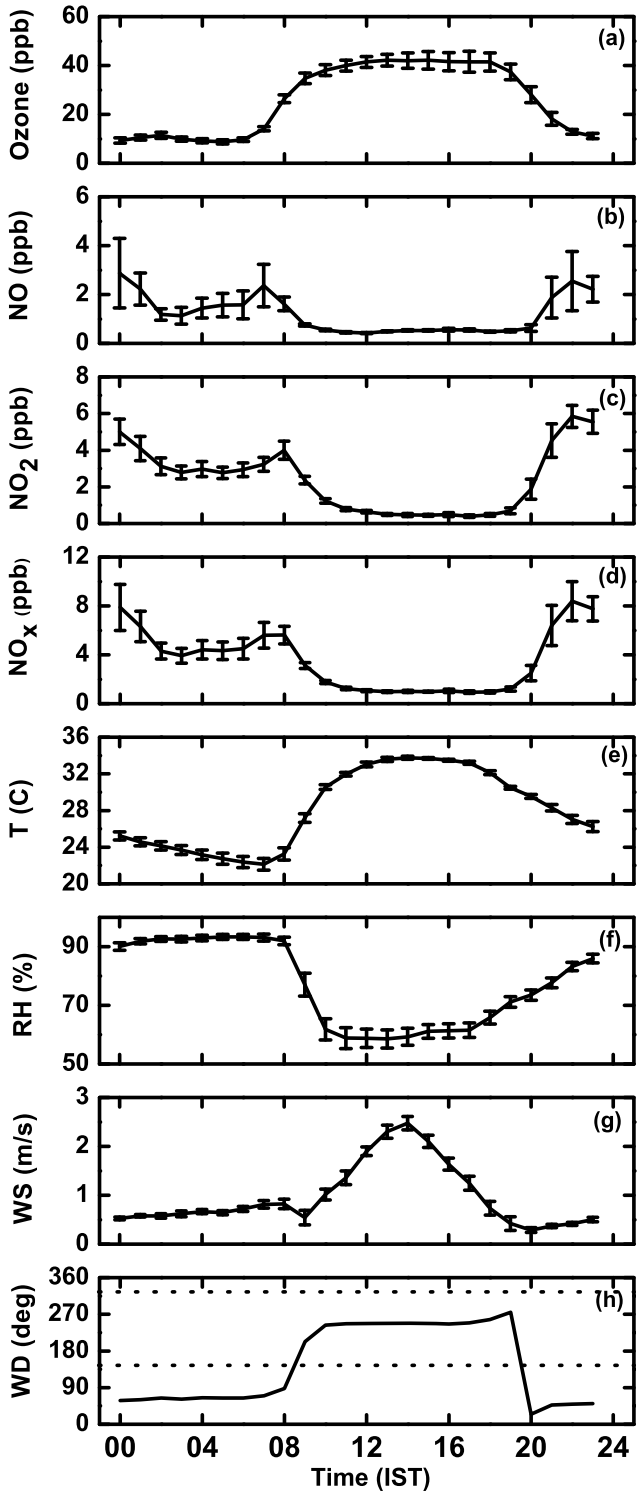

Figure 4. A typical diurnal pattern of (a) ozone, (b) NO, (c) NO_2, and (d) NO_x concentrations; (e) temperature; (f) relative humidity; (g) wind speed (WS); and (h) wind direction (WD). The wind direction between the dashed lines in Figure 4h represents the SB.

the landmass on the eastern side of the observation site (in contrast to other seasons, when it came from the ocean). This air mass brought to the site polluted continental air, which was rich in NO_x. This was manifested as a prominent increase in nighttime NO_x since a strong SB prevailed at the site during daytime and photochemistry was active. In this context, it should be noted that even though rainfall was strong from September to November (Figures 2 and 6), daytime ozone and nighttime NO_x showed high values, indicating the influence of long-range transport.

[17] The nighttime NO_x concentration, which was <3 ppb during monsoon season and <5 ppb in summer months, increased to ~6–10 ppb during the winter. Moreover, convective activities and turbulent mixing were weak during the winter (leading to lower boundary layer height), which resulted in confinement of pollutants near the surface, thus increasing their concentration levels. In addition, biomass burning in the southern peninsular region is at a maximum during this season [*Galanter et al.*, 2000], causing transport of precursors over to the observation site. During March, winds were weak (Figure 3), and the airflow pattern as well as origin of air mass back trajectories started to change. During summer, the trajectories originated over the marine environment and traversed a smaller area of landmass. But solar irradiance was at maximum and photochemistry was stronger during these months. Hence, the observed ozone concentration during summer months could be attributable mainly to photochemistry. However, the strong convective activity that is characteristic of summer enabled mixing of ozone and precursors to higher levels, thereby causing dilution of pollutants near the surface. During monsoon season, winds were strong in a westerly-southwesterly direction, back trajectories were of oceanic origin, and marine air mass prevailed over the Indian subcontinent. Marine air mass was relatively clean compared to the continental type, which was affected by human activities [*Xu et al.*, 1997; *Chan et al.*, 1998; *Saito et al.*, 2002]. In addition, the cloudy conditions reduced the solar irradiance, decreasing the day-night contrast in temperature and suppressing the photochemistry. Washout processes by heavy rains also had an effect during monsoon season. Over several locations in the Asian region, ozone showed low concentration during this period owing to the inflow of clean maritime air mass [*Lam et al.*, 2001; *Chou et al.*, 2006].

[18] Figure 6 also indicates significant differences in ozone concentrations from 2007–2008 to 2008–2009. The seasonal mean ozone concentration was found to be highest during winter 2008–2009, reaching values as high as 40 ppb, with the nighttime level of NO_x being 4–5 ppb. It was higher by ~10 ppb than that of winter 2007–2008. Ozone concentration of summer 2009 was also substantially higher compared to that of summer 2008 (by ~15 ppb). The difference in the ozone concentrations in these 2 years was examined in light of the meteorological conditions that prevailed during the 2007–2009 period. The rainfall during monsoon season (June to November) of 2007 and 2008, which are periods prior to the 2007–2008 and 2008–2009 winters, respectively, was examined (at this tropical site June to November is generally regarded as the rainy season, as can be seen in Figure 2 and as is discussed in section 2). The monsoon of 2007 (not shown in Figure 2) was very active, with a total rainfall of 1525 mm, compared to the monsoon of 2008, which had 1281 mm of rainfall. The washout of ozone precursors by continuous rain and associated high moisture content (RH >90%) could be the reason for the reduced near-surface ozone during winter 2007.

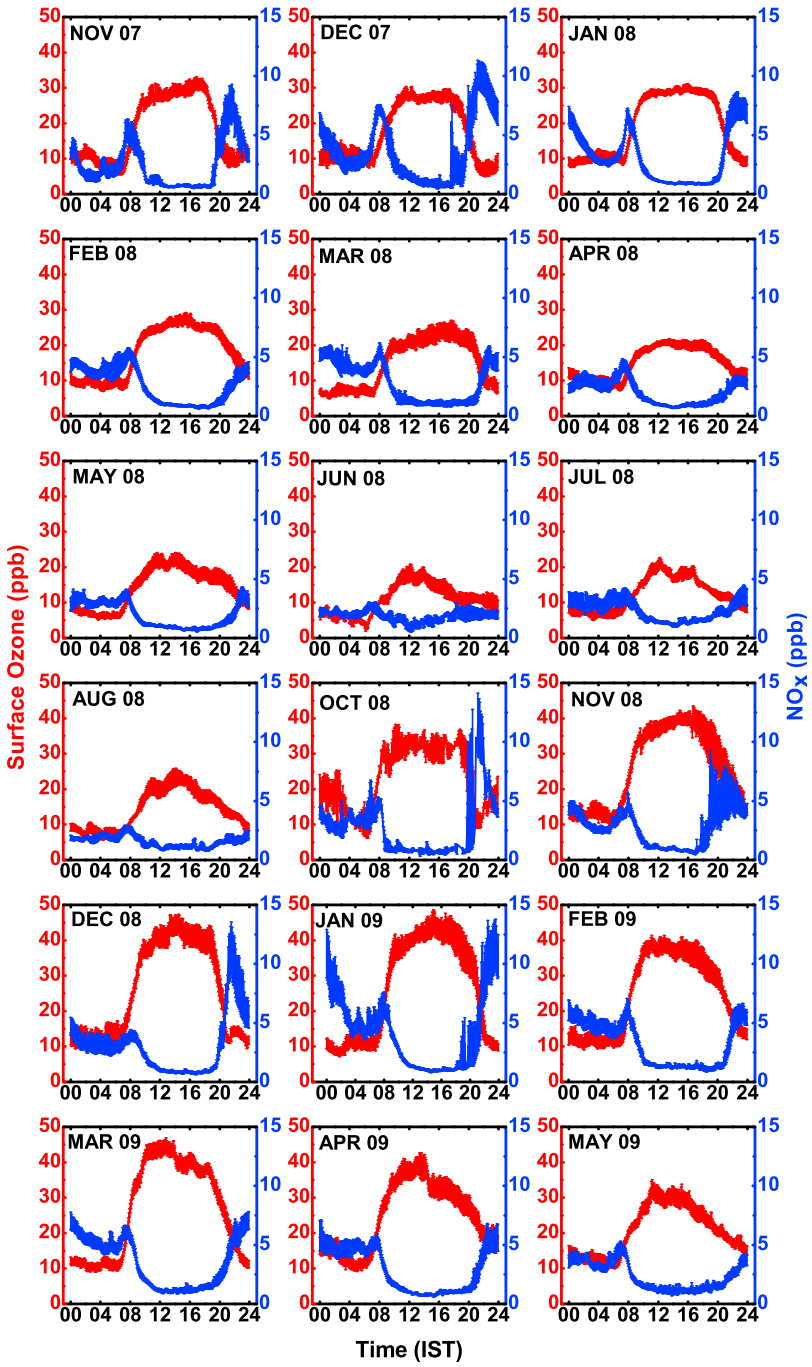

Figure 5. The monthly averaged diurnal patterns of (red) surface ozone and (blue) NO_x concentrations.

The monthly mean temperature was also significantly higher (by ~2°) during 2008–2009 compared to that of 2007–2008 (Figure 2), which again indicates the possibility of higher photochemical production of ozone during the 2008–2009 period. But ozone levels in winter (2008–2009) and summer (2009) are comparable (with daytime maximum falling in the range of 40–42 ppb). The seasonal pattern of ozone observed during the 1997–1998 period at this location showed maximum ozone concentrations during summer with slightly lower values in winter [*Nair et al.*, 2002]. These peak values were lower than those observed during 2009 but higher than those recorded in 2008. This shows that at this location the annual peak in ozone can occur during summer or winter. While the summer peak is decided by photochemistry, the winter peak is attributable to long-range transport of precursors from the inland locations. The peaks that appear in winter indicate an increase in the accumulation of NO_x, as discussed above.

4.3. Surface Ozone and NO_x Relationship

[19] Several studies have shown that morning production and evening-nighttime destruction rates of ozone are pro-

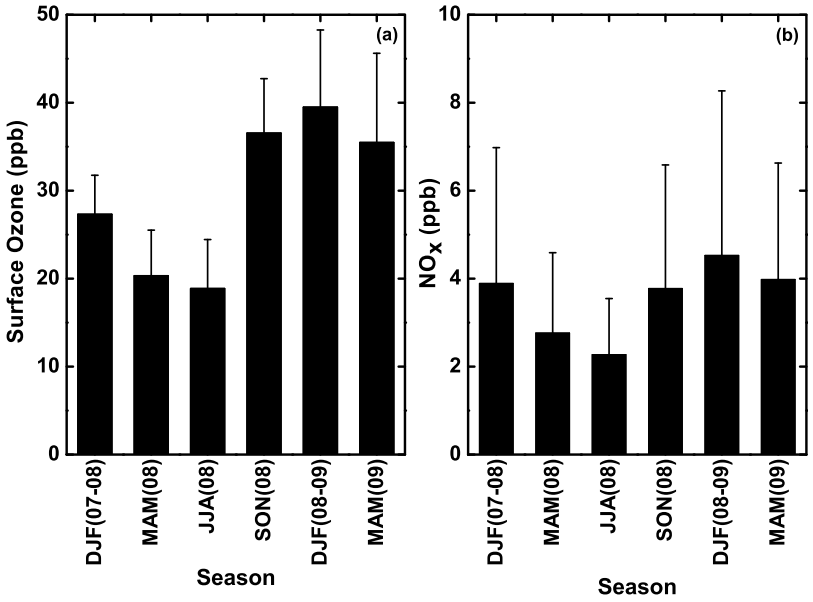

Figure 6. The seasonal mean (a) daytime ozone and (b) nighttime NO_x concentrations.

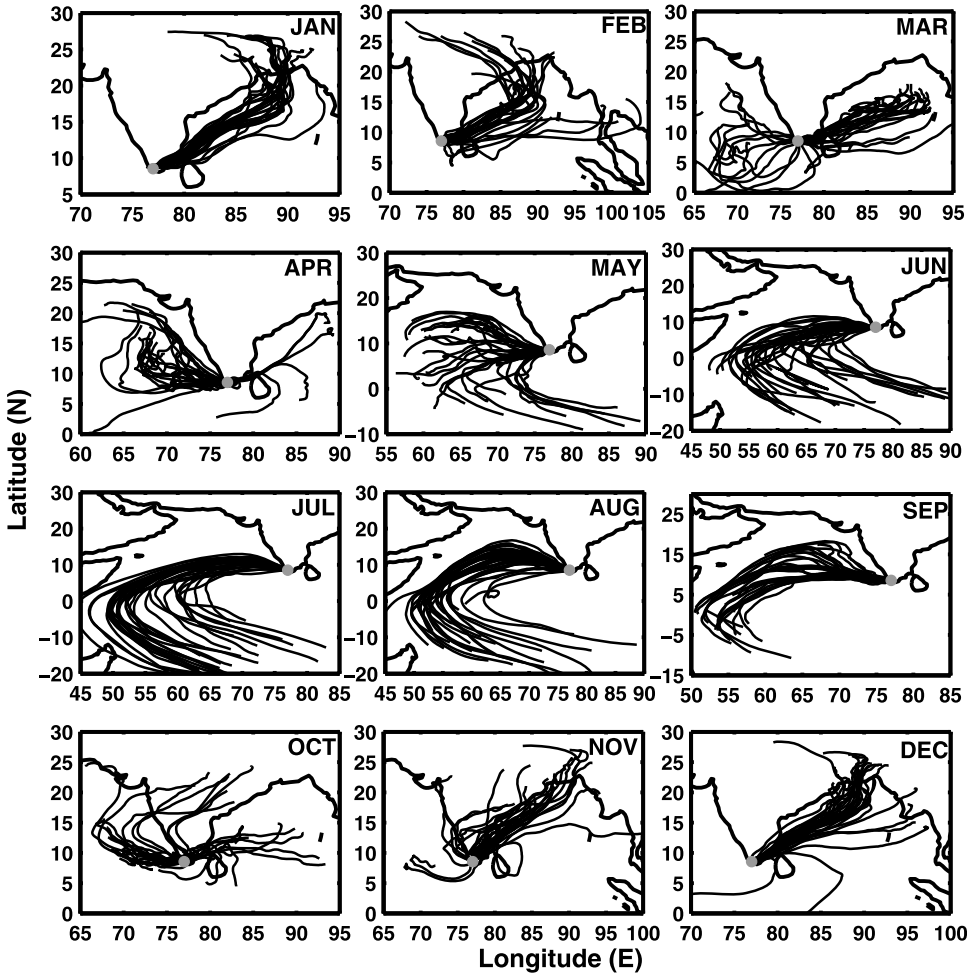

Figure 7. The 7 day air mass back trajectories reaching the observation site at 200 m at 0600 UT, obtained using the HYSPLIT model developed at NOAA's Air Resources Laboratory (R. R. Draxler and G. D. Rolph, 2003, http://ready.arl.noaa.gov/HYSPLIT.php) for the year 2008.

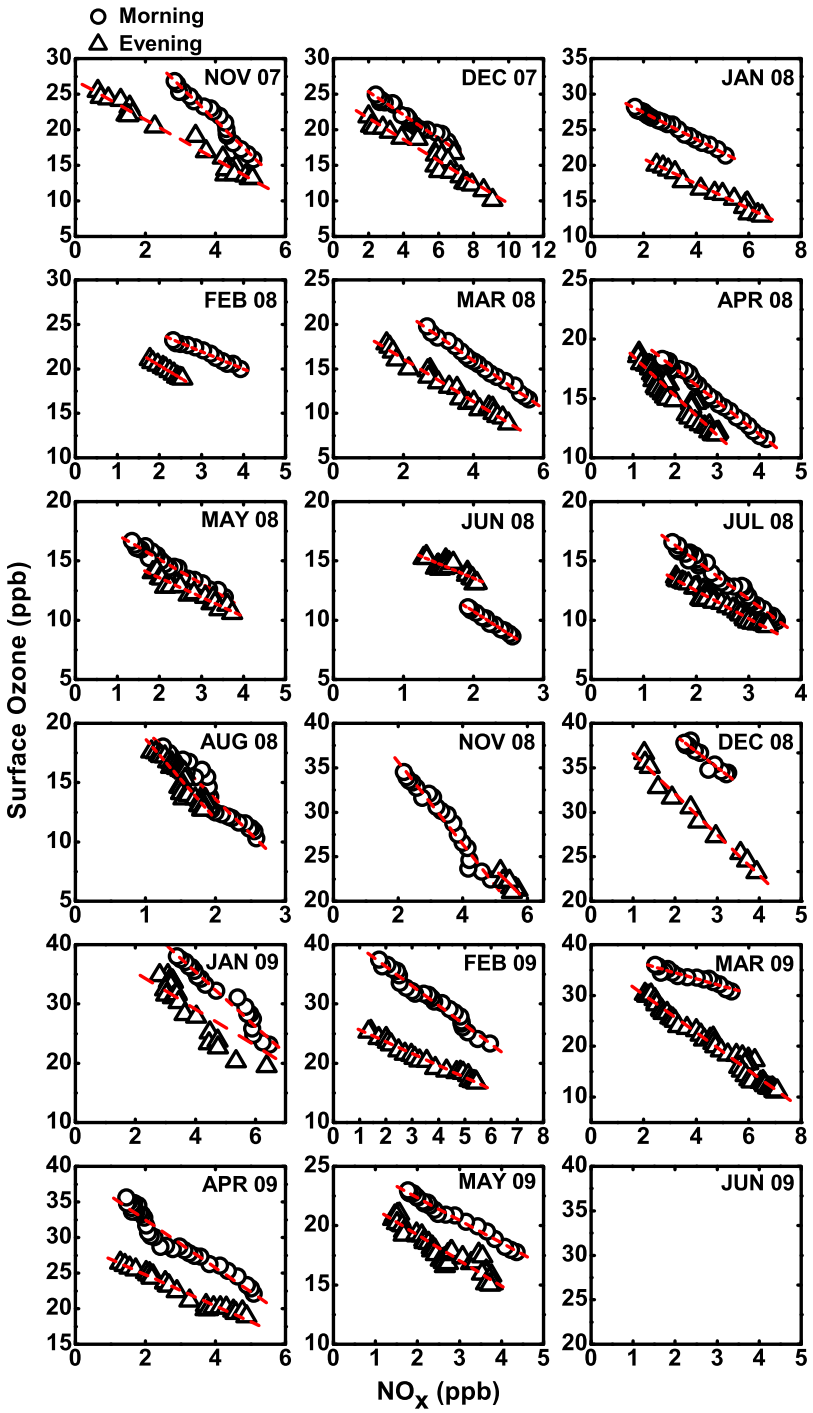

Figure 8. The monthly variation of NO_x against surface ozone for morning (circles) and evening (triangles). The straight line in each plot represents the best fit line.

portional to the NO_x concentration [*Chameides and Walker*, 1973]. All the diurnal patterns in Figure 5 show a decrease of NO_x associated with a morning increase in ozone. Similarly, an evening decrease in ozone is associated with a buildup of NO_x. The ozone and NO_x data that correspond to these periods (morning and evening) are separated from the monthly mean diurnal data (Figure 5). Figure 8 shows the variation of NO_x against ozone for morning (0900–1655 LT) and evening (1700–0855 LT) on a monthly basis (represented by different symbols). The straight line in each plot represents the best fit line obtained by linear regression analysis. Table 1 lists the correlation coefficient, y intercept, slope, and standard deviation for morning and evening on a monthly basis. In all cases, ozone and NO_x were negatively corre-

Table 1. The Correlation Coefficient, *y* Intercept, Slope, and Standard Deviation for Morning and Evening on a Monthly Basis for Surface Ozone and NO_x[a]

	Morning				Evening			
Month	*r*	Intercept	Slope	SD	*r*	Intercept	Slope	SD
Nov 2007	−0.982	40.383	−4.765	0.229	−0.989	26.936	−2.766	0.095
Dec 2007	−0.984	28.611	−1.633	0.064	−0.956	24.638	−1.502	0.106
Jan 2008	−0.997	31.169	−1.875	0.030	−0.988	24.371	−1.739	0.075
Feb 2008	−0.989	27.827	−1.961	0.091	−0.996	26.033	−2.826	0.082
Mar 2008	−0.998	26.833	−2.723	0.045	−0.988	20.908	−2.395	0.085
Apr 2008	−0.993	23.037	−2.760	0.065	−0.968	21.901	−3.329	0.127
May 2008	−0.988	19.246	−2.056	0.073	−0.964	16.847	−1.635	0.120
Jun 2008	−0.997	18.284	−3.769	0.098	−0.888	18.444	−2.450	0.260
Jul 2008	−0.989	21.521	−3.249	0.084	−0.977	17.204	−2.355	0.074
Aug 2008	−0.958	25.250	−5.818	0.356	−0.928	25.458	−6.771	0.479
Sep 2008								
Oct 2008								
Nov 2008	−0.982	45.014	−4.649	0.208	−0.879	42.162	−3.712	0.821
Dec 2008	−0.957	45.881	−3.615	0.366	−0.990	38.369	−3.419	0.160
Jan 2009	−0.978	53.828	−4.600	0.236	−0.957	41.497	−3.096	0.178
Feb 2009	−0.987	42.830	−3.268	0.111	−0.989	27.625	−2.000	0.063
Mar 2009	−0.955	39.124	−1.458	0.126	−0.989	37.623	−3.727	0.079
Apr 2009	−0.970	39.193	−3.361	0.152	−0.982	29.163	−2.195	0.085
May 2009	−0.994	26.164	−1.906	0.049	−0.952	23.549	−2.162	0.099

[a]The correlation coefficient has a significance level of $p = 0.01$.

lated with a correlation coefficient of >0.88, having a significance level of $p = 0.01$. In general, slopes are higher during the morning, indicating relatively faster increase or buildup of ozone compared to the rate of decrease in the evening. In other words, production processes are faster than processes of destruction. Alternatively, during the evening hours mesoscale transport processes could be a contributing factor. This possibility is discussed in detail in section 4.4. The intercepts show relatively low values during monsoon season, which are probably attributable to the less active photochemistry. During the months in which evening slopes were higher (February, April, and August 2008 and March 2009), the winds were weak or undergoing transition (Figure 3).

[20] The dependence of ozone on NO_x and NO_2 is further investigated by examining the monthly mean daytime values of ozone in conjunction with nighttime concentrations of NO_x. Figure 9a shows the variation of monthly mean daytime ozone along with that of nighttime NO_x, and Figures 9b and 9c show scatterplots of surface ozone with NO_2 and NO_x, respectively. The straight lines in Figures 9b and 9c represent the best fit obtained through linear regression analysis. Obviously, the daytime concentration of ozone is positively correlated with nighttime NO_x and NO_2 with the respective correlation coefficients being 0.86 and 0.77, which is significant at a 99% confidence level. There is no clear-cut dependence of ozone on NO, which remained rather steady (not shown). The interdependence of ozone and NO_2 and NO_x can be expressed through the following linear relation:

$$[\text{Ozone}] = 9.2[NO_2] + 6.1, \quad (4)$$

$$[\text{Ozone}] = 7.7[NO_x] + 2.1. \quad (5)$$

This relation suggests that one molecule of NO_x or NO_2 is responsible for the formation of seven to nine molecules of ozone. A similar rate of production is reported from rural sites in China, Germany, and the United States [*Trainer et al.*, 1993; *Volz-Thomas et al.*, 1993; *Olszyna et al.*, 1994; *Cheung and Wang*, 2001].

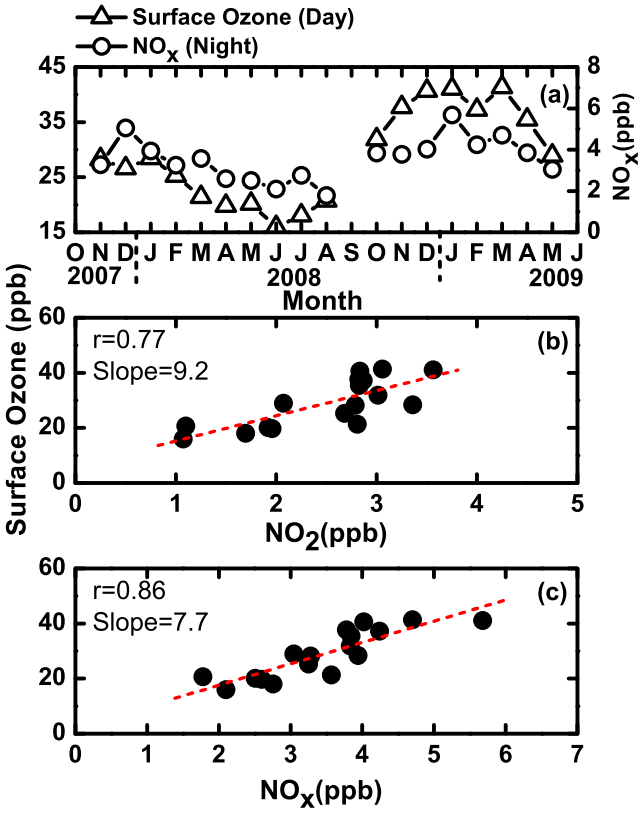

Figure 9. (a) The variation of monthly mean daytime surface ozone along with that of nighttime NO_x and scatterplots of surface ozone with (b) NO_2 and (c) NO_x.

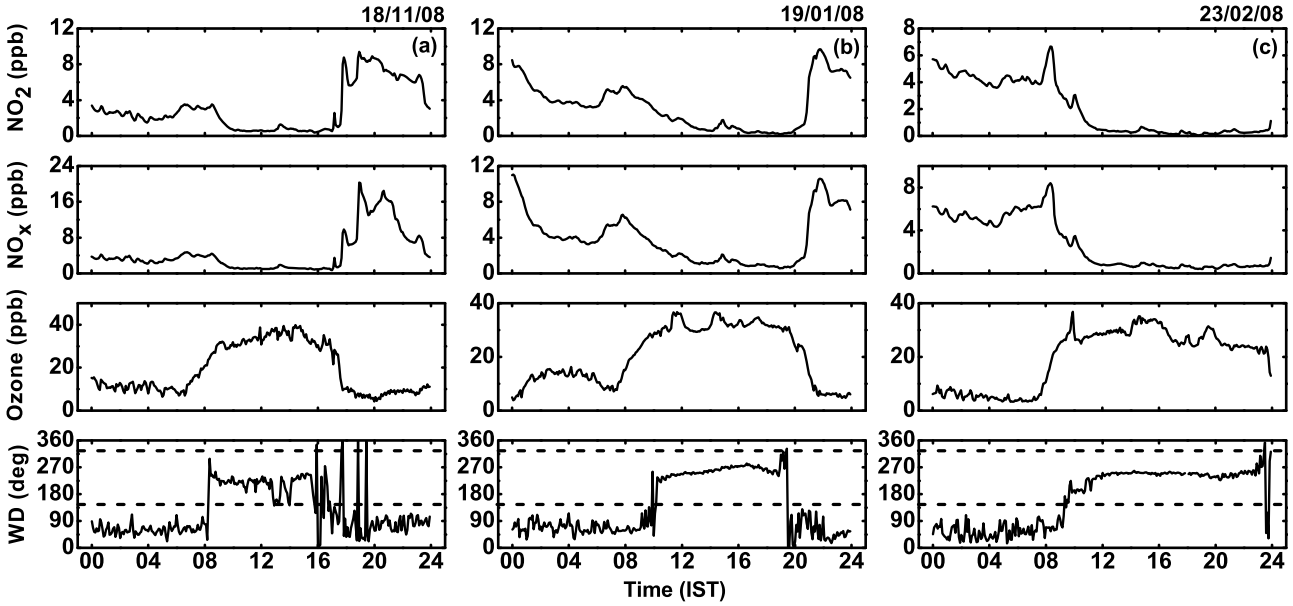

Figure 10. Typical cases of land breeze onset (a) early at ~1700 LT, (b) at ~1900 LT, and (c) late at 2300 LT.

4.4. Meteorological Effects on Temporal Variation of Surface Ozone and NO_x

4.4.1. Sea Breeze–Land Breeze Effect on Diurnal Patterns of Ozone and NO_x

[21] Being situated very close to the seacoast (coastline lies along the 145°–325° azimuth), the study site experiences persistent SB and LB activity throughout the year [*Narayanan*, 1967; *Moorthy et al.*, 1991]. Several experimental studies have been conducted on SB-LB activity and the associated thermal internal boundary layer at this site [*Kunhikrishnan et al.*, 1993]. Onset time of SB is between 0730 and 1130 LT, with the highest probability between 0830 and 0930 LT [*Prakash et al.*, 1992]. By evening SB weakens, and LB usually sets in between 1930 and 2230 LT. The wind blowing between 145° and 325° (marked by dashed lines in Figure 4h) is considered to be SB, while the seaward wind blowing between 325° and 145° constitutes LB. In general, the duration of SB is about 11 h [*Prakash et al.*, 1992]. A close association is observed between diurnal variations of ozone and NO_x and SB-LB activity. The onset of SB and morning increase in ozone occur around the same time, probably because both of these processes are driven by solar radiation. It is interesting to note that photochemistry weakens by afternoon but ozone concentration continues to be high until the onset of LB (even after sunset). Figure 10 shows three typical cases of LB onset: early at ~1700 LT (Figure 10a), at ~1900 LT (Figure 10b), and late at 2300 LT (Figure 10c). On all these days the evening-nighttime decrease in ozone coincides with the onset of LB and an increase in NO_x. It is established that SB activity is associated with a return flow aloft from warm land completing the circulation (called the SB cell). Inland penetration of SB at the observation site has been extensively studied using sodar, tower-based meteorological instruments, as well as model simulations. The vertical extent of the SB cell is ~1 km during the summer monsoon and about 800 m during the postmonsoon [*Prakash et al.*, 1992; *Kunhikrishnan et al.*, 1993; *Rani et al.*, 2010], with the landward extent of SB being only 30–50 km as it is restricted by the presence of a mountain range about 30 km southeast of the observation site. This inland region also includes rural areas where no significant sources of ozone and precursors exist. The extended peak in ozone concentration even after sunset can be attributed to two factors: (1) photochemically produced ozone is recirculated within the SB cell and (2) the major depletion mechanism of ozone during nighttime is titration by NO_x [*Jenkin and Clemitshaw*, 2000]. Because the site is very close to the seacoast and there are no major sources of NO_x present in the vicinity, the NO_x needed for titration becomes active only with the onset of LB, which brings in the polluted air from the interior landmass (in the absence of major anthropogenic activities). Diurnal patterns of ozone measured during the 1997–1998 period showed a decreasing trend by late evening and then a less prominent (secondary) peak associated with the onset of LB [*Nair et al.*, 2002]. A few months of data on NO_x measured at this location during 1998 showed values as high as 15–20 ppb, whereas the values observed for the present study ranged from 5 to 12 ppb. Probably because of the electrification of railways and the implementation of several other pollution control measures, NO_x values over this site may have decreased during the past few years. Hence, titration of ozone by NO_x occurred only after the onset of LB. In addition to this gas phase reaction, dry deposition also causes a reduction of the ozone level in the boundary layer during nighttime [*Ripperton and Vukovich*, 1971]. The low boundary layer height and reduced vertical mixing during the night lead to more ozone deposition on the surface and reduced concentration close to the ground. Among these, the gas phase chemistry dominates [*Vukovich*, 1973].

[22] The high levels of NO_x observed during nighttime are closely linked with the onset of LB, as can be seen in

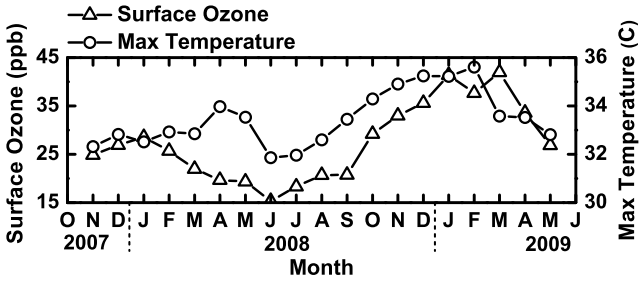

Figure 11. A plot of monthly mean daytime surface ozone and maximum temperature.

Figure 10. In addition, they are linked with other boundary layer characteristics. At this observation site the nocturnal boundary layer is shallower than its daytime counterpart by a factor of ~3 [*Kunhikrishnan et al.*, 1993], confining the pollutants to lower altitudes. As wind speed is also low during the night (Figure 4g), there is a rapid reduction in the ventilation coefficient (the product of boundary layer height and mean wind speed in the boundary layer), which restricts the dispersion of gases and other pollutants. This results in the confinement of NO_x to lower regions of the atmosphere, leading to an increase in concentration.

4.4.2. Effect of Temperature and Water Vapor on Surface Ozone and NO_x

[23] On a diurnal basis (Figures 4a and 4e) ozone shows a positive correlation with temperature, which is a measure of the intensity of incident solar radiation and consequently of the effectiveness of photochemistry. Figure 11 shows a plot of monthly mean daytime surface ozone and the corresponding maximum temperature. Ozone is positively correlated with temperature, with a coefficient of ~0.77. The positive relationship between ozone concentration and temperature is well established and explained on a theoretical basis [*Dueñas et al.*, 2002; *Tu et al.*, 2007]. A large amount of experimental evidence exists that shows the positive correlation of ozone and temperature [*Wolff and Lioy*, 1978; *Clark and Karl*, 1982; *Tu et al.*, 2007].

[24] Water vapor content in the atmosphere also plays a crucial role in the production and destruction of ozone. Since RH depends on temperature and is anticorrelated (Figures 4e and 4f), in the present study the absolute water vapor content is examined instead of RH. From simultaneous measurements of temperature and RH, water vapor content (ρ_v) (g m^{-3}) can be estimated using the following empirical relation [*Kneizys et al.*, 1980]:

$$\rho_s = A \exp\left(18.9766 - 14.9595A - 2.4388A^2\right), \quad (6)$$

$$A = T_o/(T_o + t),$$

$$T = T_o + t,$$

$$\rho_v = \rho_s(\mathrm{RH}/100)[1 - (1 - \mathrm{RH}/100)(\rho_s R_v T/P)]^{-1}, \quad (7)$$

where ρ_s is the saturation density of water vapor at ambient temperature, T_o = 273.15 K, t is temperature in °C, R_v is the gas constant for water vapor (4.615×10^{-3} mbar g m^{-3} K^{-1}), and P is the total pressure in mbar. Figure 12 shows the monthly variation of daytime ρ_v along with surface ozone. It can be seen that decrease in ozone is associated with increase of ρ_v in the atmosphere. During the monsoon season ρ_v naturally increases to very high values (23 g m^{-3}) as marine air mass with high water vapor content prevails over the region. This can cause depletion of ozone through reactions involving OH radicals, for which water vapor is the source.

4.5. Comparison of Monthly Surface Ozone With Other Locations in India

[25] Diurnal patterns of near-surface ozone with a noontime or afternoon high and a nighttime low are widely observed features at urban sites [*Trainer et al.*, 1993, 1995; *Volz-Thomas et al.*, 1993; *Kleinman et al.*, 1994; *Olszyna et al.*, 1994; *Wang et al.*, 2001; *Saito et al.*, 2002; *Tu et al.*, 2007]. Measurements made at the urban sites of Ahmedabad [*Lal et al.*, 2000] and Delhi [*Jain et al.*, 2005] exhibit symmetric diurnal variations in ozone centered at noontime. At the high-altitude location of Mount Abu ozone shows a double-hump structure in summer and spring [*Naja et al.*, 2003], due to the influence of transported ozone-rich air. At another high-altitude location, Nainital, the diurnal pattern does not show the signature of daytime photochemical buildup of ozone. Instead, it shows a slight decrease after sunrise [*Kumar et al.*, 2010]. The diurnal pattern of ozone at the industrialized inland location of Pune shows distinct variation over the year [*Beig et al.*, 2007]. The daytime peak vanishes during July and August, and from January to March the nighttime ozone concentration is significantly high. In contrast to the daytime peaks recorded at many of these other locations, the daytime peak measured at the observation site was broader, with a more or less steady value, and extended until late at night (even after sunset), which we attribute to the strong SB-LB activity at this coastal site, as discussed in section 4.4.1. While the diurnal pattern is governed by mesoscale features like SB-LB activity, the seasonal pattern depends to a certain extent on the synoptic-scale airflow and long-range transport. Table 2 shows the monthly mean minimum and maximum concentrations of surface ozone measured at different Indian sites. The maximum monthly mean ozone concentration at Trivandrum is lower than that of the other locations but comparable with that of Tranquebar, a tropical station on the east coast. The monthly minimum among all the locations is observed at Trivandrum.

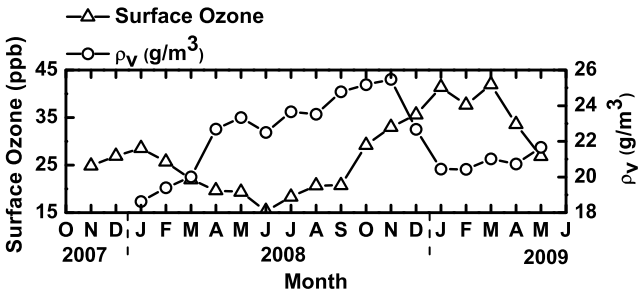

Figure 12. A plot of the monthly variation of daytime water vapor content (ρ_v) along with surface ozone.

Table 2. The Monthly Mean Minimum and Maximum Concentrations of Surface Ozone Measured at Different Indian Sites

Location	Surface Ozone (ppb)	Period of Study	References
Nainital (29.4°N, 79.5°E)	24.9 ± 8.4 to 67.2 ± 14.2	Oct 2006 to Dec 2008	*Kumar et al.* [2010]
Delhi[a] (28.7°N, 77.2°E)	(50–82) to (62–95)	Since 1997	*Jain et al.* [2005]
Mt. Abu (24.6°N, 72.7°E)	25.1 ± 9.4 to 48.8 ± 7.7	1993–2000	*Naja et al.* [2003]
Ahmedabad[a] (23°N, 72.6°E)	16.8 ± 4.2 to 51.4 ± 10.9	1991–1995	*Lal et al.* [2000]
Pune (18.5°N, 73.8°E)	12.2 to 54.6	Jun 2003 to May 2004	*Beig et al.* [2007]
Anantapur (14.6°N, 77.7°E)	26.2 ± 3.5 to 48.9 ± 7.7	Jan 2002 to Dec 2003	*Reddy et al.* [2008]
Gadanki (13.5°N, 79.2°E)	18.1 ± 10.8 to 33.6 ± 20.6	1993–1996	*Naja et al.* [2002]
Tranquebar (11°N, 79.9°E)	17 ± 7 to 23 ± 9	May 1997 to Oct 2000	*Debaje et al.* [2003]
Trivandrum (8.5°N, 77°E)	11.5 ± 4.7 to 28.1 ± 16.2	Nov 2007 to May 2009	Present study

[a]Monthly average maximum daytime concentration.

4.6. Comparison of Seasonal Variation of Surface, Tropospheric, and Total Ozone

[26] A comparative study making use of the satellite data discussed in section 3 was also carried out on the seasonal variations of near-surface ozone, tropospheric ozone, tropospheric NO_2, and total ozone. The data corresponding to the grid containing the observation site were used. Total column ozone and tropospheric NO_2 data are available on a daily basis, and tropospheric ozone data are available for 1–2 d $month^{-1}$, owing to limitations in the collocated data from MLS and OMI. The monthly averaged near-surface ozone and tropospheric ozone are shown in Figures 13a and 13b, respectively. These two patterns are more or less consistent with low values from June through September and increasing values from October onward, reaching maxima during winter and summer. But the peak in tropospheric ozone during summer (March–May) is more pronounced than that of surface ozone, and the winter (December–February) peak is more prominent for near-surface ozone. Figure 13c shows the monthly mean tropospheric NO_2 (precursor of ozone) exhibiting a seasonal pattern similar to that of tropospheric ozone. A positive correlation between tropospheric ozone and NO_2 is clearly visible in the scatterplot in Figure 13e, which shows a correlation coefficient of ~0.81 after removing the seasonal cycle. The monthly mean total ozone (Figure 13d) shows a different picture. It increased from the month of March or April, reached a maximum in May, remained high until September, and decreased in October, reaching a minimum during the winter months. This seasonal pattern is associated with strong photochemical activity combined with vertical transport processes characteristic of the tropics and is well understood [*Staehelin et al.*, 2001]. It has been established that the tropics is a region of intense photochemistry and strong vertical motion of air masses associated with convective activity [*Holton et al.*, 1995]. The vertical motions enable the mixing and transport of trace gases and aerosols from the lower troposphere into the upper troposphere and lower stratosphere (UTLS) region. Recent studies on the climatology of vertical winds at altitudes of 4–22 km at the tropical site of Gadanki (13.5°N, 79.2°E) using the mesosphere-stratosphere-troposphere radar have shown that the months from April to September are characterized by strong vertical winds in the UTLS region [*Thampi et al.*, 2009]. The reduction in tropospheric ozone, surface ozone, and tropospheric NO_2 during this period (Figures 13a to 13c) may be partly associated with this strong vertical motion. In addition, during this period winds are westerly-southwesterly, which brings in the marine air mass (discussed in section 4.2). It is also seen that the low surface ozone from March to May is associated with an increase in tropospheric ozone, which could be due to convective activity that lifts the surface ozone to higher levels. The months of April and May are also characterized by high NO_2. In this context, it should be noted that lightning is one of the sources of tropospheric NO_2, and in this region lightning is reported to be high in April and May and in October and November [*Das et al.*, 2007]. The period from October to March, when updrafts are weak or downdrafts are strong in the UTLS region [*Thampi*

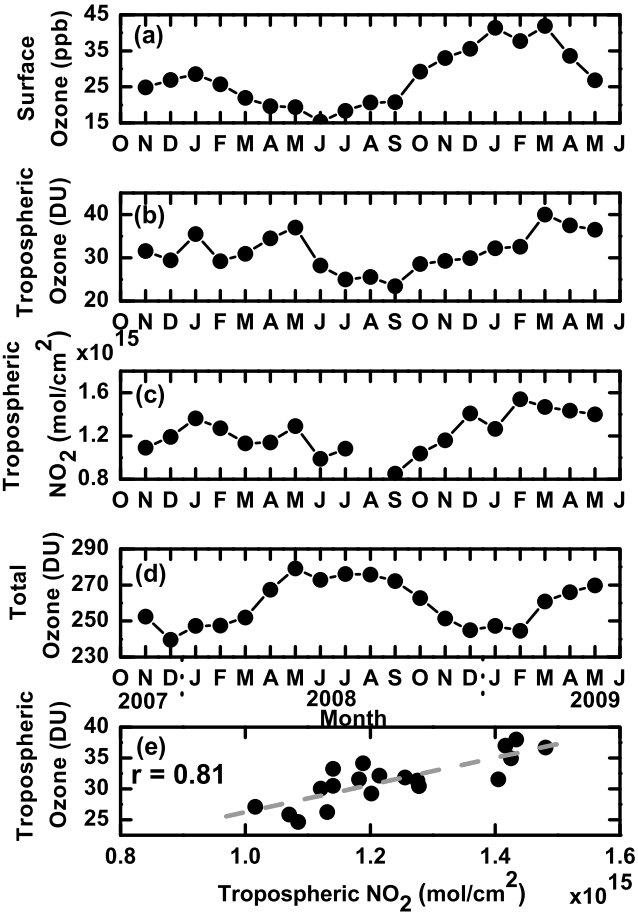

Figure 13. The monthly averaged (a) near-surface ozone, (b) tropospheric ozone (measured in Dobson units), (c) tropospheric NO_2, and (d) total ozone and (e) a scatterplot of tropospheric ozone with tropospheric NO_2.

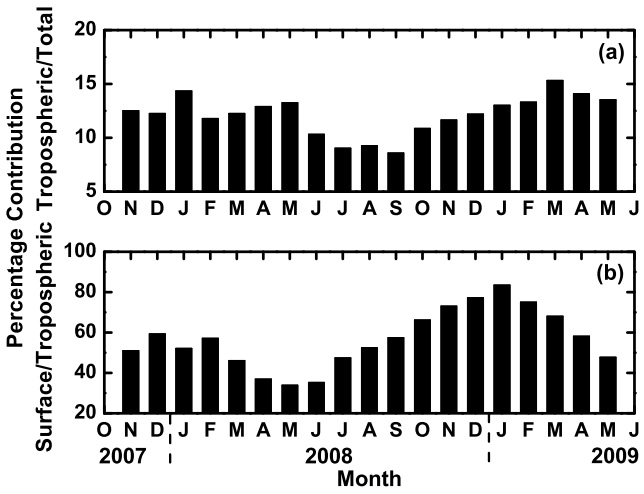

Figure 14. Percentage contribution of (a) tropospheric to total ozone and (b) surface to tropospheric ozone.

et al., 2009], is one of overall increase in tropospheric and surface ozone.

[27] Figure 14 shows the percentage contribution of tropospheric ozone to total ozone and that of surface ozone to tropospheric ozone on a month-to-month basis. Tropospheric ozone contribution to total column ozone varies from 8% to 15% over a year, with the minimum observed during the June–September period. Here it should be noted that the error in the tropospheric column ozone is ~7 DU, which includes the offset of 2 DU [*Ziemke et al.*, 2009], and the estimated standard deviation in monthly mean total column ozone is 3–9 DU. Applying the theory of propagation of errors, the estimated error in the percentage of contribution lies in the range of 14%–26%, with the maximum error observed during monsoon months and the minimum error observed in summer months. The measured surface ozone level can be considered to represent the concentration level in the atmospheric boundary layer owing to its well-mixed nature. The present analysis shows large variations (34%–83%) in the contribution of boundary layer ozone to total tropospheric column ozone. Minimum contribution is observed during summer and monsoon months. The percentage error in this case was found to be in the range 1%–8% except for the month of May, when it was 10%–12%.

5. Conclusion

[28] In this paper, the diurnal, monthly, and seasonal variations of ozone observed at the tropical coastal site of Trivandrum between November 2007 and May 2009 are presented in the light of corresponding variations in the precursor NO_x and the mesoscale and synoptic meteorological conditions. Contributions of near-surface ozone to tropospheric ozone and that of tropospheric ozone to total columnar ozone have also been estimated by analysis of satellite data. Major observations are summarized below.

[29] 1. The diurnal variation of ozone shows a broad daytime peak extending from ~1000 LT to late evening and reaching a minimum during the night. The daytime peak is attributed to strong photochemical production of ozone from precursors and also to mesoscale circulations such as sea breeze and land breeze. The daytime peak of ozone extends until the onset of land breeze, which brings in the NO_x necessary for titration of ozone to occur.

[30] 2. High nighttime concentration of NO_x is due to the prevailing LB circulation and the shallow nighttime boundary layer.

[31] 3. The amplitudes and durations of peaks in ozone vary with season. Daytime ozone and nighttime NO_x peak during postmonsoon and winter months. On the other hand, nighttime ozone and daytime NO_x remain more or less steady for all the seasons. Seasonal variations are associated with changes in synoptic wind patterns, as revealed by airflow patterns and air mass back trajectories.

[32] 4. Even though photochemistry is strong during the summer months, turbulent mixing transports ozone and precursors to higher levels, thereby causing dilution of pollutants near the surface. During the monsoon season synoptic wind is westerly-southwesterly, bringing in pristine marine air masses and thus reducing the ozone concentration.

[33] 5. The concentration of daytime ozone is positively correlated with that of nighttime NO_x on a monthly basis. The present analysis reveals that one molecule of NO_x or NO_2 is responsible for the production of seven to nine molecules of ozone at the surface level.

[34] 6. On a monthly basis, daytime ozone is positively correlated with maximum temperature and negatively correlated with absolute water vapor content.

[35] 7. Tropospheric ozone and NO_2 show similar seasonal patterns. Tropospheric ozone contributes 8%–15% of total ozone over the observation site. Near-surface ozone contributes 34%–83% of tropospheric ozone, with the maximum contribution occurring during the winter months of December, January, and February.

[36] **Acknowledgments.** This study forms part of the ATCTM project under ISRO GBP. The authors gratefully acknowledge the Meteorological Facility of the Vikram Sarabhai Space Centre for providing surface meteorological data for this study. The Dutch-Finnish-built OMI is part of the NASA EOS Aura satellite payload. The OMI project is managed by NIVR and KNMI in the Netherlands. The OMI NO_2 data were provided by http://avdc.nasa.gov/.

References

Aneja, V. P., D. Kim, and W. L. Chameides (1997), Trends and analysis of ambient NO, NO_y, CO, and ozone concentrations in Raleigh, North Carolina, *Chemosphere*, *34*, 611–623, doi:10.1016/S0045-6535(96)00393-1.

Asnani, G. C. (1993), Climatology of the tropics, in *Tropical Meteorology*, vol. 1, pp. 100–204, Indian Inst. of Trop. Meteorol., Pune, India.

Beig, G., S. Gunthe, and D. B. Jadhav (2007), Simultaneous measurements of ozone and its precursors on a diurnal scale at a semi-urban site in Pune, *J. Atmos. Chem.*, *57*, 239–253, doi:10.1007/s10874-007-9068-8.

Cárdenas, L. M., J. F. Austin, R. A. Burgess, K. C. Clemitshaw, S. Dorling, S. A. Penkett, and R. M. Harrison (1998), Correlations between CO, NO_y, O_3 and non-methane hydrocarbons and their relationships with meteorology during winter 1993 on the North Norfolk Coast, U.K., *Atmos. Environ.*, *32*, 3339–3351, doi:10.1016/S1352-2310(97)00445-7.

Carpenter, L. J., P. S. Monks, B. J. Bandy, and S. A. Penkett (1997), A study of peroxy radicals and ozone photochemistry at coastal sites in the northern and southern hemispheres, *J. Geophys. Res.*, *102*(D21), 25,417–25,427, doi:10.1029/97JD02242.

Celarier, E. A., et al. (2008), Validation of Ozone Monitoring Instrument nitrogen dioxide columns, *J. Geophys. Res.*, *113*, D15S15, doi:10.1029/2007JD008908.

Chameides, W. L. (1978), The photochemical role of tropospheric nitrogen oxides, *Geophys. Res. Lett.*, *5*, 17–20, doi:10.1029/GL005i001p00017.

Chameides, W., and J. C. G. Walker (1973), A photochemical theory of tropospheric ozone, *J. Geophys. Res.*, *78*(36), 8751–8760, doi:10.1029/JC078i036p08751.

Chameides, W., and J. C. G. Walker (1976), A time-dependent photochemical model for ozone near the ground, *J. Geophys. Res.*, *81*, 413–420, doi:10.1029/JC081i003p00413.

Chameides, W. L., P. S. Kasibhatla, J. Yienger, and H. Levy (1994), Growth of continental scale Metro-Agro-Plexes, regional ozone pollution and world food production, *Science*, *264*, 74–77, doi:10.1126/science.264.5155.74.

Chameides, W. L., et al. (1999a), Is ozone pollution affecting crop yields in China?, *Geophys. Res. Lett.*, *26*, 867–870, doi:10.1029/1999GL900068.

Chameides, W. L., et al. (1999b), Case study of the effects of atmospheric aerosols and regional haze on agriculture: An opportunity to enhance crop yields in China though emission controls?, *Proc. Natl. Acad. Sci. U. S. A.*, *96*, 13,626–13,633, doi:10.1073/pnas.96.24.13626.

Chan, L. Y., H. Y. Liu, K. S. Lam, and T. Wang (1998), Analysis of seasonal behaviour of tropospheric ozone at Hong Kong, *Atmos. Environ.*, *32*, 159–168, doi:10.1016/S1352-2310(97)00320-8.

Chatterton, T., S. Dorling, A. Lovett, and M. Stephenson (2000), Air quality in Norwich, UK: Multi-scale modeling to assess the significance of city, county and regional pollution sources, *Environ. Monit. Assess.*, *65*, 425–433, doi:10.1023/A:1006477112407.

Cheung, V. T. F., and T. Wang (2001), Observational study of ozone pollution at a rural site in the Yangtze Delta of China, *Atmos. Environ.*, *35*, 4947–4958, doi:10.1016/S1352-2310(01)00351-X.

Chou, C. C. K., S. C. Liu, C. Y. Lin, C. J. Shiu, and K. H. Chang (2006), The trend of surface ozone in Taipei, Taiwan, and its causes: Implications for ozone control strategies, *Atmos. Environ.*, *40*, 3898–3908, doi:10.1016/j.atmosenv.2006.02.018.

Clark, T. L., and T. R. Karl (1982), Application of prognostic meteorological variables to forecasts of daily maximum one hour ozone concentrations in the northeastern United States, *J. Appl. Meteorol.*, *21*, 1662–1671, doi:10.1175/1520-0450(1982)021<1662:AOPMVT>2.0.CO;2.

Comrie, A. C., and B. Yarnal (1992), Relationships between synoptic-scale atmospheric circulation and ozone concentrations in metropolitan Pittsburgh, Pennsylvania, *Atmos. Environ.*, *26B*, 301–312.

Crutzen, P. J. (1974), Photochemical reactions initiated by and influencing ozone in unpolluted tropospheric air, *Tellus*, *26*, 47–57, doi:10.1111/j.2153-3490.1974.tb01951.x.

Crutzen, P. J. (1995), Ozone in the troposphere, in *Composition, Chemistry and Climate of the Atmosphere*, edited by H. B. Singh, pp. 349–393, Van Nostrand Reinhold, New York.

Crutzen, P. J., L. E. Heidt, J. P. Krasnec, W. H. Pollock, and W. Seiler (1979), Biomass burning as a source of atmospheric gases CO, H_2, N_2O, CH_3Cl and COS, *Nature*, *282*, 253–256, doi:10.1038/282253a0.

Crutzen, P. J., A. C. Delany, J. Greenberg, P. Haagenson, L. Heidt, R. Leub, W. Pollock, W. Seiler, A. Wartburg, and P. Zimmerman (1985), Tropospheric chemical composition measurements in Brazil during the dry season, *J. Atmos. Chem.*, *2*, 233–256, doi:10.1007/BF00051075.

Crutzen, P. J., M. G. Lawrence, and U. Poschl (1999), On the background photochemistry of tropospheric ozone, *Tellus, Ser. A*, *51*, 123–146, doi:10.1034/j.1600-0870.1999.t01-1-00010.x.

Danalatos, D., and S. Glavas (1996), Diurnal and seasonal variations of surface ozone in a mediterranean coastal site, Patras, Greece, *Sci. Total Environ.*, *177*, 291–301, doi:10.1016/0048-9697(95)04928-2.

Danielsen, E. F. (1959), The laminar structure of the atmosphere and its relation to the concept of a tropopause, *Meteorol. Atmos. Phys.*, *11*, 293–332, doi:10.1007/BF02247210.

Das, S. M., S. Sampath, and G. Mohankumar (2007), Lightning hazard in Kerala, *J. Mar. Atmos. Res.*, *3*(1), 111–117.

Debaje, S. B., S. Johnson Jeyakumar, K. Ganesan, D. B. Jadhav, and P. Seetaramayya (2003), Surface ozone measurements at tropical rural coastal station Tranquebar, India, *Atmos. Environ.*, *37*, 4911–4916, doi:10.1016/j.atmosenv.2003.08.005.

Dueñas, C., M. C. Fernández, S. Cañete, J. Carretero, and E. Liger (2002), Assessment of ozone variations and meteorological effects in an urban area in the Mediterranean coast, *Sci. Total Environ.*, *299*, 97–113, doi:10.1016/S0048-9697(02)00251-6.

Elminir, H. K. (2005), Dependence of urban air pollutants on meteorology, *Sci. Total Environ.*, *350*, 225–237, doi:10.1016/j.scitotenv.2005.01.043.

Finnan, J. M., J. I. Burke, and M. B. Jones (1997), An evaluation of indices that describe the impact of ozone on the yield of spring wheat (Triticum aestivum L.), *Atmos. Environ.*, *31*, 2685–2693, doi:10.1016/S1352-2310(97)00105-2.

Fishman, J., and P. J. Crutzen (1977), A numerical study of tropospheric photochemistry using a one dimensional model, *J. Geophys. Res.*, *82*, 5897–5906, doi:10.1029/JC082i037p05897.

Fishman, J., and P. J. Crutzen (1978), The origin of ozone in the troposphere, *Nature*, *274*, 855–858, doi:10.1038/274855a0.

Fishman, J., S. Solomon, and P. J. Crutzen (1979), Observational and theoretical evidence in support of a significant in-situ photochemical source of tropospheric ozone, *Tellus*, *31*, 432–446, doi:10.1111/j.2153-3490.1979.tb00922.x.

Fishman, J., K. Fakhruzzaman, B. Cros, and D. Nganga (1991), Identification of widespread pollution in the Southern Hemisphere deduced from satellite analyses, *Science*, *252*, 1693–1696, doi:10.1126/science.252.5013.1693.

Galanter, M., M. Levy II, and G. R. Carmichael (2000), Impacts of biomass burning on tropospheric CO, NO_x and O_3, *J. Geophys. Res.*, *105*, 6633–6653, doi:10.1029/1999JD901113.

Ghude, S. D., S. L. Jain, B. C. Arya, G. Beig, Y. H. Ahammed, A. Kumar, and B. Tyagi (2008), Ozone in tha ambient air at a tropical megacity, Delhi: Characteristics, trends and cumulative ozone exposure indices, *J. Atmos. Chem.*, *60*(3), 237–252, doi:10.1007/s10874-009-9119-4.

Heck, W. W., O. C. Taylor, R. Adams, G. Bingham, J. Miller, E. Preston, and L. Weinstein (1982), Assessment of crop loss from ozone, *J. Air Pollut. Control Assoc.*, *32*, 353–356.

Holton, J. R., P. H. Haynes, M. E. McIntyre, A. R. Douglass, R. B. Rood, and L. Pfister (1995), Stratosphere-troposphere exchange, *Rev. Geophys.*, *33*, 403–439, doi:10.1029/95RG02097.

Intergovernmental Panel on Climate Change (2007), *Climate Change 2007: The Physical Science Basis. Contribution of Working Group I to the Fourth Assessment Report of the Intergovernmental Panel on Climate Change*, edited by S. Solomon et al., Cambridge Univ. Press, Cambridge, U. K.

Jaffe, D. A., R. E. Honrath, L. Zhang, H. Akimoto, A. Shimizu, H. Mukai, K. Murano, S. Hatakeyama, and J. Merrill (1996), Measurements of NO, NO_y, CO, and O_3 and estimation of the ozone production rate at Oki Island, Japan, during PEM-West, *J. Geophys. Res.*, *101*, 2037–2048, doi:10.1029/95JD01699.

Jain, S. L., B. C. Arya, A. Kumar, S. D. Ghude, and P. S. Kulkarni (2005), Observational study of surface ozone at New Delhi, India, *Int. J. Remote Sens.*, *26*(16), 3515–3524, doi:10.1080/01431160500076616.

Jenkin, M. E., and K. C. Clemitshaw (2000), Ozone and other secondary photochemical pollutants: Chemical processes governing their formation in the planetary boundary layer, *Atmos. Environ.*, *34*, 2499–2527, doi:10.1016/S1352-2310(99)00478-1.

Khemani, L. T., G. A. Momin, P. S. P. Rao, R. Vijayakumar, and P. D. Safai (1995), Study of surface ozone behaviour at urban and forested sites in India, *Atmos. Environ.*, *29*(16), 2021–2024, doi:10.1016/1352-2310(94)00293-T.

Kleinman, L., et al. (1994), Ozone formation at a rural site in the south eastern United States, *J. Geophys. Res.*, *99*, 3469–3482, doi:10.1029/93JD02991.

Kneizys, F. X., E. P. Shettle, W. O. Gallery, J. H. Chetwynd Jr., L. W. Abreu, J. E. A. Selby, R. W. Fenn, and R. A. McClatchey (1980), Atmospheric transmittance/radiance: Computer code LOWTRAN 5, *Environ. Res. Pap.*, *697*, 217–219.

Kumar, R., M. Naja, S. Venkataramani, and O. Wild (2010), Variations in surface ozone at Nainital: A high-altitude site in the central Himalayas, *J. Geophys. Res.*, *115*, D16302, doi:10.1029/2009JD013715.

Kunhikrishnan, P. K., K. S. Gupta, R. Ramachandran, W. J. Prakash, and K. N. Nair (1993), Study on thermal internal boundary layer structure over Thumba, India, *Ann. Geophys.*, *11*, 52–60.

Lal, S., M. Naja, and B. H. Subbaraya (2000), Seasonal variations in surface ozone and its precursors over an urban site in India, *Atmos. Environ.*, *34*, 2713–2724, doi:10.1016/S1352-2310(99)00510-5.

Lam, K. S., T. J. Wang, L. Y. Chan, T. Wang, and J. Harris (2001), Flow patterns influencing the seasonal behaviour of surface ozone and carbon monoxide at a coastal site near Hong Kong, *Atmos. Environ.*, *35*, 3121–3135, doi:10.1016/S1352-2310(00)00559-8.

Lee, D. S., M. K. Holland, and N. Falla (1996), The potential impact of ozone on materials in the UK, *Atmos. Environ.*, *30*, 1053–1065, doi:10.1016/1352-2310(95)00407-6.

Lehman, J., K. Swinton, S. Bortnick, C. Hamilton, E. Baldridge, B. Eder, and B. Cox (2004), Spatio-temporal characterization of tropospheric ozone across the eastern United States, *Atmos. Environ.*, *38*, 4357–4369, doi:10.1016/j.atmosenv.2004.03.069.

Levy, H., II (1971), Normal atmosphere: Large radical and formaldehyde concentrations predicted, *Science*, *173*, 141–143, doi:10.1126/science.173.3992.141.

Lin, X., M. Trainer, and S. C. Liu (1988), On the nonlinearity of the tropospheric ozone production, *J. Geophys. Res.*, *93*, 15,879–15,888, doi:10.1029/JD093iD12p15879.

Logan, J. A., J. J. Prather, S. C. Wofsy, and M. B. McElroy (1981), Tropospheric chemistry: A global perspective, *J. Geophys. Res.*, *86*, 7210–7254, doi:10.1029/JC086iC08p07210.

Michelsen, H. A., R. J. Salawitch, P. O. Wennberg, and J. G. Anderson (1994), Production of $O(^1D)$ from photolysis of O_3, *Geophys. Res. Lett.*, *21*(20), 2227–2230, doi:10.1029/94GL02052.

Moorthy, K. K., P. B. Nair, and B. V. Krishna Murthy (1991), Size distribution of coastal aerosols: Effects of local sources and sinks, *J. Appl. Meteorol.*, *30*, 844–852, doi:10.1175/1520-0450(1991)030<0844:SDOCAE>2.0.CO;2.

Nair, P. R., D. Chand, S. Lal, K. S. Modh, M. Naja, K. Parameswaran, S. Ravindran, and S. Venkataramani (2002), Temporal variations in surface ozone at Thumba (8.6°N, 77°E)-a tropical coastal site in India, *Atmos. Environ.*, *36*, 603–610, doi:10.1016/S1352-2310(01)00527-1.

Naja, M., and S. Lal (2002), Surface ozone and precursor gases at Gadanki (13.5°N, 79.2°E), a tropical rural site in India, *J. Geophys. Res.*, *107*(D14), 4197, doi:10.1029/2001JD000357.

Naja, M., S. Lal, and D. Chand (2003), Diurnal and seasonal variabilities in surface ozone at a high altitude site Mt Abu (24.6°N, 72.7°E, 1680m asl) in India, *Atmos. Environ.*, *37*, 4205–4215, doi:10.1016/S1352-2310(03)00565-X.

Narayanan, V. (1967), An observational study of sea-breeze at an equatorial coastal station, *Indian J. Meteorol. Geophys.*, *18*, 497–504.

Olszyna, K. J., E. M. Bailey, R. Simonaitis, and J. F. Meagher (1994), Ozone and NO_y relationships at a rural site, *J. Geophys. Res.*, *99*(D7), 14,557–14,563, doi:10.1029/94JD00739.

Olszyna, K. J., M. Luria, and J. F. Meagher (1997), The correlation of temperature and rural ozone levels in southeastern U.S.A., *Atmos. Environ.*, *31*, 3011–3022, doi:10.1016/S1352-2310(97)00097-6.

Prakash, J. W. J., R. Ramachandran, K. N. Nair, K. Sen Gupta, and P. K. Kunhikrishnan (1992), On the structure of sea-breeze fronts observed near the coastline of Thumba, India, *Boundary Layer Meteorol.*, *59*, 111–124, doi:10.1007/BF00120689.

Raddatz, R. L., and J. D. Cummine (2001), Temporal surface ozone patterns in urban Manitoba, Canada, *Boundary Layer Meteorol.*, *99*, 411–428, doi:10.1023/A:1018983012168.

Rani, S. I., R. Ramachandran, D. B. Subrahamanyam, D. P. Alappattu, and P. K. Kunhikrishnan (2010), Characterization of sea/land breeze circulation along the west coast of Indian sub-continent during pre-monsoon season, *Atmos. Res.*, *95*, 367–378, doi:10.1016/j.atmosres.2009.10.009.

Reddy, R. R., K. R. Gopal, L. S. S. Reddy, K. Narasimhulu, K. R. Kumar, Y. N. Ahammed, and C. V. K. Reddy (2008), Measurements of surface ozone at semi-arid site Anantapur (14.62°N, 77.65°E, 331 m asl) in India, *J. Atmos. Chem.*, *59*, 47–59, doi:10.1007/s10874-008-9094-1.

Reich, P. B., and R. G. Amundson (1985), Ambient levels of ozone reduce net photosynthesis in tree and crop species, *Science*, *230*, 566–570, doi:10.1126/science.230.4725.566.

Reiter, E. R. (1975), Stratospheric-tropospheric exchange processes, *Rev. Geophys.*, *13*(4), 459–474, doi:10.1029/RG013i004p00459.

Ripperton, L. A., and F. M. Vukovich (1971), Gas phase destruction of tropospheric ozone, *J. Geophys. Res.*, *76*(30), 7328–7333, doi:10.1029/JC076i030p07328.

Saito, S., I. Nagao, and H. Tanaka (2002), Relationship of NO_x and NMHC to photochemical O_3 production in a coastal and metropolitan areas of Japan, *Atmos. Environ.*, *36*, 1277–1286, doi:10.1016/S1352-2310(01)00557-X.

Staehelin, J., N. R. P. Harris, C. Appenzeller, and J. Eberhard (2001), Ozone trends: A review, *Rev. Geophys.*, *39*(2), 231–290, doi:10.1029/1999RG000059.

Stull, R. B. (1988), *An Introduction to Boundary Layer Meteorology*, Kluwer Acad., Boston, Mass.

Thampi, B. V., S. V. Sunilkumar, and K. Parameswaran (2009), Lidar studies of particulates in the UTLS region at a tropical station over the Indian subcontinent, *J. Geophys. Res.*, *114*, D08204, doi:10.1029/2008JD010556.

Trainer, M., et al. (1993), Correlation of ozone with NO_y in photochemically aged air, *J. Geophys. Res.*, *98*(D2), 2917–2925, doi:10.1029/92JD01910.

Trainer, M., B. A. Ridley, M. P. Buhr, G. Kok, J. Walega, G. Hübler, D. D. Parrish, and F. C. Fehsenfeld (1995), Regional ozone and urban plumes in the southeastern United States: Birmingham, a case study, *J. Geophys. Res.*, *100*(D9), 18,823–18,834, doi:10.1029/95JD01641.

Tu, J., Z.-G. Xia, H. Wang, and W. Li (2007), Temporal variations in surface ozone and its precursors and meteorological effects at an urban site in China, *Atmos. Res.*, *85*, 310–337, doi:10.1016/j.atmosres.2007.02.003.

Volz-Thomas, A., et al. (1993), Photo-oxidants and precursors at Schauinsland, Black Forest, A contribution to subproject TOR, in *Photo-oxidants: Precursors and Products: Proceedings of EUROTRAC Symposium '92, Garmisch-Partenkirchen, Federal Republic of Germany 23rd–27th March 1992*, edited by P. M. Borrell et al., pp. 98–103, SPB Acad., The Hague, Netherlands.

Vukovich, F. M. (1973), Some observations of the variations of ozone concentrations at night in the North Carolina Piedmont boundary layer, *J. Geophys. Res.*, *78*(21), 4458–4462, doi:10.1029/JC078i021p04458.

Vukovich, F. M. (1994), Boundary layer ozone variations in the eastern United States and their association with meteorological variations: Long-term variations, *J. Geophys. Res.*, *99*(D8), 16,839–16,850, doi:10.1029/93JD02554.

Vukovich, F. M. (1995), Regional-scale boundary layer ozone variations in the eastern United States and their association with meteorological variations, *Atmos. Environ.*, *29*(17), 2259–2273, doi:10.1016/1352-2310(95)00146-P.

Wang, T., V. T. F. Cheung, M. Anson, and Y. S. Li (2001), Ozone and related gaseous pollutants in the boundary layer of eastern China: Overview of the recent measurements at a rural site, *Geophys. Res. Lett.*, *28*(12), 2373–2376, doi:10.1029/2000GL012378.

Weinstock, B., and H. Niki (1972), Carbon monoxide balance in nature, *Science*, *176*, 290–292, doi:10.1126/science.176.4032.290.

Wofsy, S. C., J. C. McConnell, and M. B. McElroy (1972), Atmospheric CH_4, CO, and CO_2, *J. Geophys. Res.*, *77*(24), 4477–4493, doi:10.1029/JC077i024p04477.

Wolff, G. T., and P. J. Lioy (1978), An empirical model for forecasting maximum daily ozone levels in the northeastern U.S., *J. Air Pollut. Control Assoc.*, *28*(10), 1034–1038.

World Health Organization (2000), *Guidelines for Air Quality*, 190 pp., Geneva, Switzerland.

Xu, J., Y. Zhu, and J. Li (1997), Seasonal cycles of surface ozone and NO_x in Shanghai, *J. Appl. Meteorol.*, *36*, 1424–1429, doi:10.1175/1520-0450(1997)036<1424:SCOSOA>2.0.CO;2.

Ziemke, J. R., S. Chandra, B. N. Duncan, L. Froidevaux, P. K. Bhartia, P. F. Levelt, and J. W. Waters (2006), Tropospheric ozone determined from AURA OMI and MLS: Evaluation of measurements and comparison with the Global Modeling Initiative's Chemical Transport Model, *J. Geophys. Res.*, *111*, D19303, doi:10.1029/2006JD007089.

Ziemke, J. R., S. Chandra, B. N. Duncan, M. R. Schoeberl, O. Torres, M. R. Damon, and P. K. Bhartia (2009), Recent biomass burning in the tropics and related changes in tropospheric ozone, *Geophys. Res. Lett.*, *36*, L15819, doi:10.1029/2009GL039303.

L. M. David and P. R. Nair, Space Physics Laboratory, Vikram Sarabhai Space Centre, Trivandrum 695022, Kerala, India. (prabha_nair@vssc.gov.in)